$Cu(H_2O)_2(C_2H_8N_2)SO_4$: A quasi-two-dimensional $S=\frac{1}{2}$ Heisenberg antiferromagnet

M. Kajňaková,[1] M. Orendáč,[1] A. Orendáčová,[1] A. Vlček,[1] J. Černák,[1] O. V. Kravchyna,[2] A. G. Anders,[1,2] M. Bałanda,[3] J.-H. Park,[4] A. Feher,[1] and M. W. Meisel[4]

[1]*Center of Low Temperature Physics, Faculty of Sciences, P. J. Šafárik University, Park Angelinum 9, 041 54 Košice, Slovakia*

[2]*Institute of Low Temperature Physics and Engineering, Ukrainian Academy of Sciences, Lenin Avenue 47, 310164 Kharkov, Ukraine*

[3]*Institute of Nuclear Physics, Polish Academy of Sciences, Radzikovskiego 152, 31-142 Kraków, Poland*

[4]*Department of Physics and Center for Condensed Matter Sciences, University of Florida, P. O. Box 118440, Gainesville, Florida 32611-8440, USA*

(Received 4 March 2004; revised manuscript received 27 September 2004; published 26 January 2005)

The experimental results of the susceptibility, specific heat, magnetization, and electron spin resonance of $Cu(H_2O)_2(C_2H_8N_2)SO_4$ are reported. Despite the triangular arrangement of chemical bonds, the system is identified as an $S=1/2$ Heisenberg antiferromagnet where the dominant exchange coupling $J/k_B \approx -1.4$ K is mediated by a square network of hydrogen bonds. The long-range ordering observed at $T_N=0.91$ K is proposed to be Néel type. The possibility of tuning the strength of the exchange couplings in various directions is discussed.

DOI: 10.1103/PhysRevB.71.014435 PACS number(s): 75.40.Cx, 75.50.Ee, 76.30.−v, 75.10.Dg

I. INTRODUCTION

The physical properties of a geometrically frustrated magnet represented by the Heisenberg antiferromagnet on a triangular lattice (HATL) have been extensively investigated,[1] and considerable theoretical effort has been devoted to understanding the nature of the ground state in the quantum regime. More specifically, the role of quantum spin fluctuations in suppressing the long-range order was a subject of the debate[2] generated by Anderson's proposal that the ground state is a spin liquid.[3] Recently, theoretical studies were extended to consider the so-called Row model describing a spatially anisotropic triangular antiferromagnet with different values of exchange coupling constants J_1 and J_2 in different directions (see Fig. 1). These studies[4–6] addressed the ground-state phase diagram of the Row model in zero magnetic field. Although the different calculation techniques led to slightly different phase boundaries, the phase diagram of the Heisenberg antiferromagnet on a spatially anisotropic triangular lattice possesses three clearly distinguishable regions. Specifically, a Néel-type ordered phase exists from $J_1/J_2=0$ to $J_1/J_2 \approx 1/2$, a phase with a spiral ground state is located in the region $1/2 < J_1/J_2 \lesssim 4$, and quantum disordered phases are predicted at $J_1/J_2=1/2$ and for $J_1/J_2 \gtrsim 4$.

For $S=1/2$ Heisenberg triangular magnets with pronounced quantum effects, most of the experimental effort has been devoted to the study of isotropic systems.[7–10] In contrast, there are only a few studies of $S=1/2$ HATL with strong spatial anisotropy, a notable example being θ-$(BEDT\text{-}TTF)_2RbZn(SCN)_4$,[11] a compound belonging to θ-type BEDT-TTF organic salts.[12] The systematic study of the theoretically proposed phase diagram of the Row model requires a class of materials which allow the J_1/J_2 ratio to be tuned. For example, the spatial anisotropy may be achieved by considering a chain material, where the exchange interaction along the chains is mediated by covalent bonds, while hydrogen bonds among the chains create exchange paths in the other direction. In this work, the thermodynamic quantities and electron spin resonance spectra of the title compound are reported. This material possesses the aforementioned structural features that are potentially consistent with spatial anisotropy of the exchange interaction. The analysis of the thermodynamic data and electron spin resonance (ESR) spectra confirms this expectation and supports the identification of the studied material as an $S=1/2$ Heisenberg antiferromagnet in which exchange interactions are mediated predominantly by a square network of hydrogen bonds.

II. CRYSTAL STRUCTURE AND ORBITAL INTERACTIONS

$Cu(H_2O)_2(en)SO_4$, $en=(C_2H_8N_2)$, crystallizes in the monoclinic space group $C2/c$, with unit cell parameters $a=7.232(1)$ Å, $b=11.752(2)$ Å, $c=9.768(1)$ Å, $\beta=105.50(1)°$, $Z=4$.[13] The structure is built of neutral chains running along the a axis [see Figs. 2(a) and 2(b)]. The paramagnetic Cu(II) ion is located in a distorted octahedron. The tetragonal distortion is manifested by the different bond lengths between Cu(II) ions and ligands in the equatorial plane $[Cu-N_{C_2H_8N_2}=1.984(2)$ Å, $Cu-O_{H_2O}=1.976(2)$ Å] and apical positions $[Cu-O_{SO_4}=2.498(2)$ Å]. The paramag-

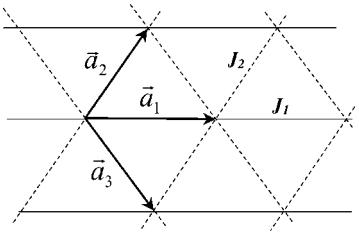

FIG. 1. Schematic plot of a triangular lattice with spatially anisotropic exchange couplings. The exchange interaction J_1 extends in the $\vec{a}_1$ direction, whereas the exchange interaction J_2 propagates along $\vec{a}_2$ and $\vec{a}_3$.

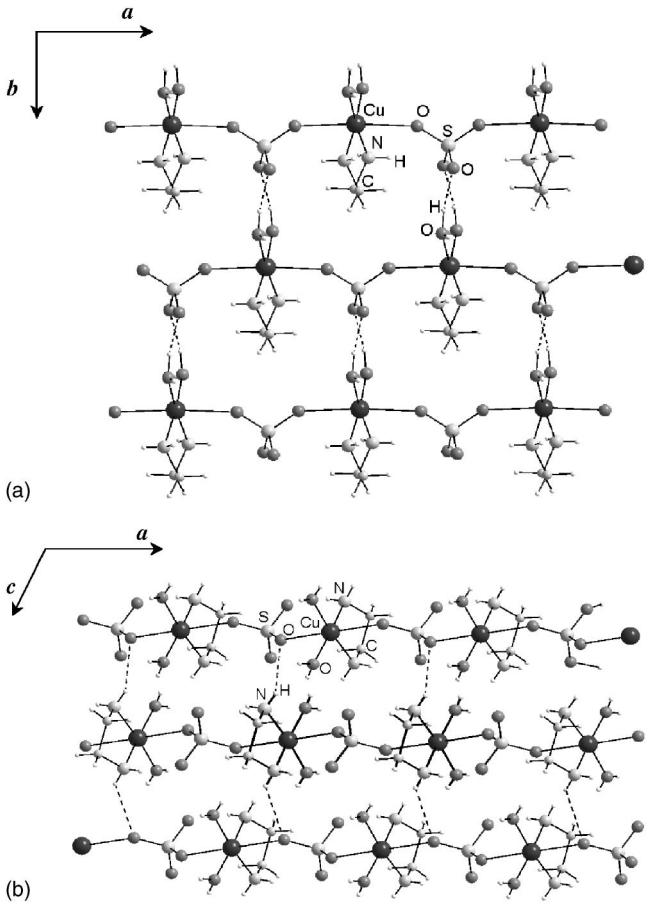

FIG. 2. Crystal structure of $Cu(H_2O)_2(en)SO_4$ in (a) *ab* and (b) *ac* planes. The chains are running along the *a* axis. The hydrogen bonds connecting the chains are denoted by dashed lines.

netic Cu(II) ions are linked by covalent bonds via a diamagnetic $[SO_4]^{2-}$ unit in the chain direction. A closer inspection of the structure reveals the presence of hydrogen bonds linking the Cu(II) ions in adjacent chains from the *ab* layer. These hydrogen bonds are located between the oxygen atoms from the $[SO_4]^{2-}$ units and the oxygen atoms from the water molecules from the neighboring chains, see Fig. 2(a). The Cu(II) ions in one chain are shifted by $(1/2,1/2)$ with respect to those from the adjacent one, thus the covalent and hydrogen bonds effectively create triangular layers with two kinds of exchange paths. Additional hydrogen bonds have also been found linking the Cu(II) ions from the adjacent layers [see Fig. 2(b)]. More specifically, the neighboring chains in the *ac* plane are linked by the hydrogen bonds between the oxygen atoms from the $[SO_4]^{2-}$ units and the nitrogen atoms from the *en* in the neighboring chains. Considering the geometrical parameters of a hydrogen bond $X-H\cdots A$ formed between *X* and *A* atoms, namely, the resulting bond lengths and angle $\angle XHA$, the hydrogen bonds between the layers are much weaker than those within the layers.[14] Although from a structural point of view the hydrogen bonds are much weaker than covalent ones, the hydrogen bonds are known to significantly influence the magnetic properties of the system.[15,16]

The resultant ratio of the exchange interactions J_1/J_2 mediated by covalent and hydrogen bonds will be significantly influenced by the symmetry of the wave function of the unpaired electron of the Cu(II) ion. For a Cu(II) ion placed in the axially deformed octahedron, the unpaired electron can be described by the wave function with either $d_{x^2-y^2}$ or d_{z^2} symmetry, where the *x* and *y* axes are defined along the Cu-O and Cu-N bonds in the equatorial plane and the *z* axis is normal to the plane. Since the lobes of the d_{z^2} orbitals are oriented along the chains, the overlap with the orbitals of appropriate symmetry from the $[SO_4]^{2-}$ group will lead to the enhancement of intrachain coupling. In contrast, the intrachain interaction is reduced if the unpaired electron is located in the $d_{x^2-y^2}$ orbital whose lobes are located in the basal plane. In this situation, the interchain exchange coupling mediated by the hydrogen bonds should be increased. Although the pronounced elongation of the octahedron revealed by the structural studies at room temperature suggests the second possibility, the corresponding low-temperature investigation of the Cu(II) environment must be performed before using this conjecture in the interpretation of the experimental data.

III. EXPERIMENTAL DETAILS

Q-band ESR ($\lambda \approx 4$ mm, $f \approx 73$ GHz) experiments were performed using a powder sample cooled between 4.2 and 20 K, where the temperature was measured to ± 0.1 or ± 0.5 K, below and above 15 K, respectively. A spherical sample with a diameter of about 1 mm was formed by using GE 7031 varnish and was placed in the cylindrical cavity resonator operating in the TE_{013} mode.

Static magnetic susceptibility and magnetization measurements of powdered samples were performed in a commercial superconducting quantum interference device magnetometer. The susceptibility studies were performed in a magnetic field of 1 kG while the temperature was varied from 2 to 300 K, whereas the dominant part of magnetization work was done at 1.8, 5, and 10 K, while varying the field from 0 to 50 kG. More detailed analysis of the data required subsequent magnetization measurements at 1.8 K up to 70 kG. Several small pieces of a pellet, which were obtained by pressing a powder sample, provided a total mass of 85 mg and were placed in a gelcap which was held by a straw. The diamagnetic contribution of the background, which was measured in an independent run, was subtracted from the total signal.

A Lake Shore system, Model 7225, was used for the measurements of the ac magnetic susceptibility. Both real and imaginary components were measured in the frequency range from 125 Hz to 2 kHz and the amplitude of the driving field was equal to 5 G. The measurements were conducted in the temperature range from 2 to 15 K.

Using a relaxation technique in a commercial dilution refrigerator, specific heat measurements were conducted with a 95 mg powder sample pressed in the form of a pellet. A RuO_2 thermometer, Dale RC 550 of about 4.7 kΩ,[17] was calibrated against a commercial Lake Shore thermometer, Model GR 200A-30. A silver wire, 40 μm in diameter and 7-cm long, was used as a link between the cold thermal reservoir and the platform containing the sample, thermometer, and a strain gauge heater. The specific heat measurement of a 59 mg bundle of small single crystals, each with

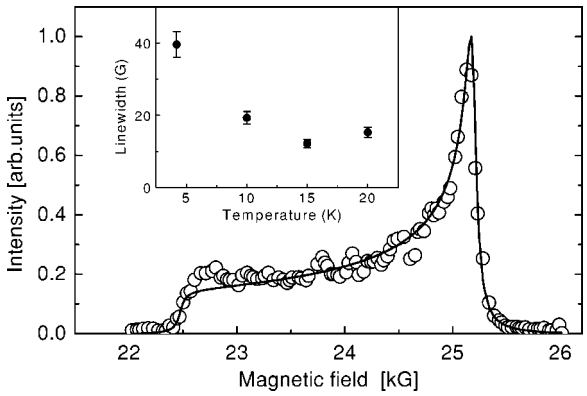

FIG. 3. Resonance spectrum of powder $Cu(H_2O)_2(en)SO_4$ studied at 4.2 K and 72.810 GHz. The solid line represents the results of a least-squares fit. Inset: temperature dependence of the linewidth of the resonance line.

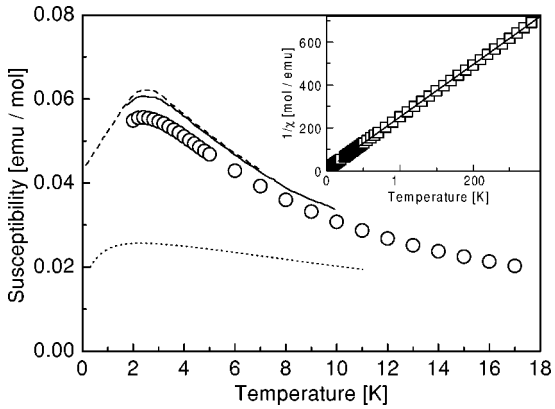

FIG. 4. Temperature dependence of the susceptibility of $Cu(H_2O)_2(en)SO_4$ (circles) at low temperatures. The theoretical prediction for a 1D Heisenberg antiferromagnetic chain with $g=2.15$, $J/k_B=-2$ K is denoted by the dashed line. The solid and dotted lines represent predictions for a spatially isotropic 2D Heisenberg antiferromagnet on a square lattice with $g=2.15$, $J/k_B=-1.3$ K and on a triangular lattice with $g=2.15$, $J/k_B=-4.4$ K, respectively. Inset: high-temperature susceptibility data (squares) analyzed using the Curie-Weiss law, and the result is given by the solid line.

approximate dimensions of $0.8\times0.2\times0.1$ mm^3, was conducted in the same experimental setup. The specific heat was measured with a maximum experimental error of about 6%.[18]

The particle size analysis was performed with a commercial device manufactured by Malvem Instruments. The distribution in the size of the grains in a typical powder sample was studied in the size range from 0.02 to 2000 μm.

IV. RESULTS AND DISCUSSION

The ESR spectra are of a form that is standard for a number of randomly oriented small single crystals, each of them reflecting the axial symmetry of the surroundings of a transition metal ion with $S=1/2$, and a typical absorption band is presented in Fig. 3. The spectrum represents a rather wide absorption band beginning from the value of the resonant magnetic field $B_\parallel$ corresponding to $g_\parallel$ of the Cu(II) magnetic ion and ending with a narrow peak at $B_\perp$ corresponding to the $g_\perp$ value.

Numerical studies of the measured ESR spectra were performed over the whole absorption band for each spectrum. In the numerical analysis, ΔB, $g_\perp$, and $g_\parallel$ were used as parameters at each temperature, and ΔB, the linewidth of the resonance line of each single crystal, was assumed to be independent of the orientation of the single crystal. The best fit was obtained when $g_\perp=2.064\pm0.002$ and $g_\parallel=2.315\pm0.003$, and to within 0.1%, these values were independent of temperature from 4.2 to 20 K. In contrast, ΔB increases significantly at the lowest temperature, see inset in Fig. 3. Since the study of the anisotropy of the g factor confirmed that the strong elongation of the octahedron prevails down to the lowest temperatures, the enhancement of the coupling via the hydrogen bonds can be expected. In addition, the steep increase of the ESR linewidth below 10 K is consistent with the development of short-range magnetic correlations.

After subtracting the core diamagnetic contribution, approximated by using Pascal's constants and found to be equal to -123.1×10^{-6} emu/mol, the susceptibility data above 15 K were fit by the Curie-Weiss law, see inset in Fig. 4. This fit yielded $g=2.09\pm0.04$ and $\theta=-3.3\pm0.1$ K, the latter confirming the presence of antiferromagnetic interactions. The behavior of the susceptibility below 15 K is characterized by a round maximum observed at 2.5 K, see Fig. 4. It should be noted that the observed temperature dependence of the magnetic susceptibility is consistent with the behavior of the linewidth of the ESR resonance line. In order to estimate how the two different exchange paths contribute to the resulting magnetic coupling, the susceptibility was analyzed in more detail.

A paramagnetic Cu(II) ion is a rather good example of a Heisenberg ion, and therefore our material can be described by the Heisenberg Hamiltonian for a triangular lattice,[4] namely,

$$\mathcal{H}=-2J_1\sum_{i,\alpha} S_i\cdot S_\alpha-2J_2\sum_{i,\beta} S_i\cdot S_\beta, \qquad (1)$$

where $\alpha=i+1$, $\beta=i+1$ for sites adjacent to the ith site in the direction of the unit vectors in the horizontal ($\vec{a}_1$) and oblique ($\vec{a}_2,\vec{a}_3$) directions, respectively. Since, to our knowledge, there are no quantum-mechanical calculations for the specific heat and the susceptibility of the Row model, the limiting models were applied for the analysis of the low-temperature susceptibility, and this approach was also applied in Ref. 19. More specifically, the susceptibility data were compared with numerical predictions for a Heisenberg chain possessing antiferromagnetic coupling[20] and with results from a high temperature series expansion for a two-dimensional (2D) Heisenberg antiferromagnet (HAF) on square[21] and triangular lattices.[22] In the analysis for each model, the value of the exchange coupling was tuned until the position of the calculated maximum of the susceptibility coincided with the one observed in the experimental data. As

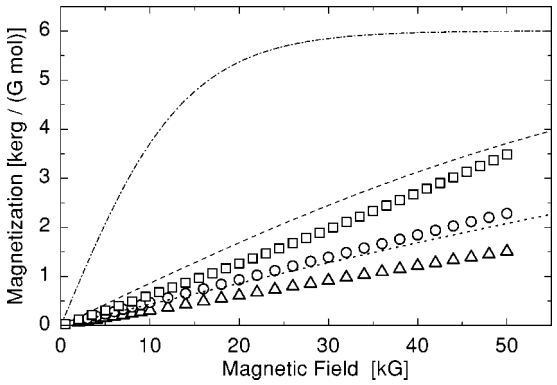

FIG. 5. Magnetic field dependence of magnetization of $Cu(H_2O)_2(en)SO_4$. The experimental data acquired at 1.8 (squares), 5 (circles), and 10 K (triangles) are compared with the corresponding predictions from the Brillouin function for 1.8 (dash-dotted line), 5 (dashed line), and 10 K (dotted line) with $g=2.15$, as obtained from the analysis of ESR data.

can be seen in Fig. 4, if we use the average g value obtained from the ESR data, i.e., $g=2.15$, the data are best reproduced by the model for a 2D HAF on a square lattice with $J/k_B=-1.3$ K. This fact may indicate that the magnetic behavior of the system may be approximated by 2D HAF on a square lattice. However, since the theoretical predictions for the HAF chain model with $g=2.15$, $J/k_B=-2$ K and for the 2D HAF on a square lattice with $g=2.15$, $J/k_B=-1.3$ K are quite similar, the identification of the system based only on the susceptibility data may be ambiguous. Nevertheless, the results suggest that $Cu(H_2O)_2(en)SO_4$ is *not* a representative of an $S=1/2$ Heisenberg magnet on a spatially isotropic triangular lattice.

It is well known that for a number of geometrically frustrated magnets, a small amount of structural disorder can induce a spin-glass transition.[1] The possible presence of a spin-glass state was experimentally explored by ac susceptibility measurements performed from 2 to 15 K. Since these ac results are independent of frequency and identical with the static measurements, the existence of a spin-glass state above 2 K seems to be unlikely.

The field dependence of the magnetization was measured up to 50 kG at 1.8, 5, and 10 K, and the results are presented in Fig. 5. The experimental data obtained at 1.8 K are characterized by upward curvature, which is absent in the data studied at higher temperatures. The magnetization data were compared with the Brillouin function describing an $S=1/2$ paramagnet with $g=2.15$ obtained from the ESR data discussed previously. The comparison confirms the presence of antiferromagnetic coupling that tends to decrease the total magnetization when compared with a paramagnetic system. More detailed analysis has been performed by comparing the numerical calculations of the magnetic field dependence of the magnetization at zero temperature and experimental data obtained at 1.8 K in magnetic fields up to 70 kG, see Fig. 6. Specifically, the calculation of the magnetization was performed with a finite HAF chain[23] and with a 2D HAF on a square lattice.[24] Since the value of the saturation magnetic field B_{sat} could not be achieved experimentally, B_{sat} was estimated in the mean field approximation as[25]

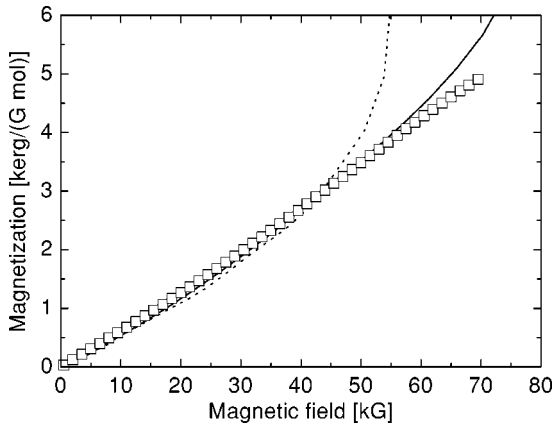

FIG. 6. Magnetic field dependence of the magnetization of $Cu(H_2O)_2(en)SO_4$ studied at 1.8 K. The experimental data (squares) are compared with the numerical predictions using $g=2.15$ calculated at zero temperature for a Heisenberg antiferromagnetic chain with saturation field $B_{sat}=55$ kG (dashed line) and for a 2D Heisenberg antiferromagnet on a square lattice with $B_{sat}=72$ kG (solid line). See text for a more detailed discussion.

$$B_{sat}=\frac{2z|J|}{g\mu_B}, \tag{2}$$

where z represents the number of the nearest neighbors and μ_B stands for the Bohr magneton. Using the values of the J and g parameters obtained from susceptibility and ESR analysis, respectively, B_{sat} was estimated to be 55 kG for the Heisenberg chain and 72 kG for the 2D HAF on a square lattice. The comparison suggests that the curvature of the experimental data is better described by the prediction for the 2D system. However, the good agreement between the prediction for the 2D system and experimental data should be interpreted with caution since mutual cancellation of finite temperature effects,[25] an inaccurate determination of B_{sat}, and the potential deviation from the behavior predicted for a 2D HAF on a square lattice cannot be ruled out.

Specific heat studies of a powder sample were conducted from nominally 100 mK to 9 K. The magnetic specific heat displays a round maximum at 1.8 K, whereas a λ-like anomaly, associated with the long-range ordering, appears at $T_N=0.91$ K, see Fig. 7. Since the compound is a magnetic insulator, only magnetic and lattice contributions are considered in the analysis. After subtracting the lattice contribution using the Debye approximation, the magnetic entropy was calculated numerically. Standard extrapolations were used to cover the whole temperature interval, and the calculation yielded 5.95 J/(K mol), which is close to the theoretical value $R\ln(2S+1)=5.76$ J/(K mol) for an $S=1/2$ system. The amount of entropy removed by short-range correlations represents about 80% of the total entropy and is strong evidence of the low-dimensional character of the magnetic correlations in this material.

The round maximum in the experimental specific heat data, which can be attributed to short-range correlations, was also analyzed using the aforementioned limiting models. The specific heat data were compared with the numerical predic-

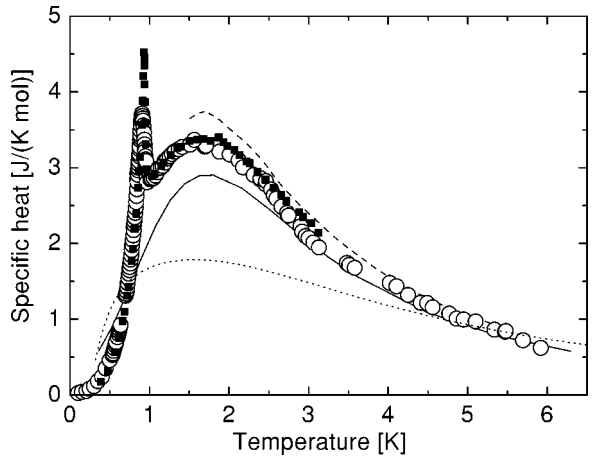

FIG. 7. Temperature dependence of magnetic specific heat of $Cu(H_2O)_2(en)SO_4$ powder (empty circles) and single crystals (full squares). The theoretical prediction for a 1D Heisenberg antiferromagnetic chain with $J/k_B=-1.8$ K is denoted by solid line. The predictions for a spatially isotropic 2D Heisenberg antiferromagnet on a square lattice with $J/k_B=-1.4$ K and on a triangular lattice with $J/k_B=-2.2$ K, are represented by the dashed and dotted lines, respectively. See text for a more detailed discussion.

tions for a HAF chain[26] and with the results from high-temperature series expansions for a 2D HAF on square[21] and triangular lattices.[22] Similarly as for the susceptibility, the comparison of the data with the prediction for an $S=1/2$ HAF on an isotropic triangular lattice confirmed that $Cu(H_2O)_2(en)SO_4$ does not represent such a system, and the behavior of the data can be better approximated by the predictions for a 1D HAF chain with $J/k_B=-1.8$ K and a 2D HAF on a square lattice with $J/k_B=-1.4$ K. The deviation of the data from the aforementioned models could be caused by several mechanisms which are discussed below.

Since the studied material magnetically orders at $T_N=0.91$ K, the effect of long-range ordering could be responsible for the observed discrepancy. Taking into account that the critical region around T_N can be confined to $|T-T_N|/T_N<10^{-1}$, which for the studied material covers the temperature range from nominally 0.8 to 1.0 K, it is obvious that the deviation persists high above the critical region. However, as confirmed by the analysis of specific heat and susceptibility of a number of prototype Heisenberg chain materials and Heisenberg antiferromagnets on square lattices, the deviations from the corresponding model predictions appear in the region where ordering occurs and at lower temperatures.[27] This observation suggests that 3D ordering effects should not have a significant influence in the region where short-range correlations are formed.

As far as single-ion effects are concerned, only anisotropy in the g factor is induced by crystal electric fields for an $S=1/2$ system. This effect is manifested in the anisotropy of exchange interaction ΔJ and a coarse estimate is $\Delta J/J=[(g_{\parallel}-g_{\perp})/g_{\mathrm{av}}]^2$, where g_{av} represents the average value of the g factor.[27] Using the results of the analysis of the ESR spectra, the anisotropy of the exchange interaction in $Cu(H_2O)_2(en)SO_4$ is estimated as $\Delta J/J\approx 0.014$. A recent quantum Monte Carlo study of an $S=1/2$ weakly anisotropic 2D HAF system on a square lattice[28] confirmed that, for 1% easy axis anisotropy and temperatures higher than $0.31J$, the specific heat data for the anisotropic and isotropic systems coincide. Consequently, the single-ion effects can be ruled out as a source of the aforementioned discrepancy.

Dipolar interactions represent another mechanism which may be considered. If the structure and type of magnetic ion are known, the estimation of the dipolar interaction is straightforward. Using the same approach as in Ref. 31, the magnitude of the dipolar coupling between adjacent layers in $Cu(H_2O)_2(en)SO_4$ is $J^{\mathrm{dip}}\approx 3$ mK. Since the magnetic specific heat originating from dipolar interactions appears only in a temperature region comparable with the magnitude of dipolar coupling,[29,30] in the studied material the resulting value of J^{dip} enables one to assume that dipolar coupling is not likely to contribute to short-range correlations at 1.8 K. Therefore, it may be stated that specific heat data in the region of the broad maximum will not be significantly influenced by dipolar interactions.

Next, the effect of the powdered nature of the sample is discussed. If the magnetic correlation length becomes comparable with the dimensions of the grains in the powder, the magnetic properties will start to deviate from those investigated on a single crystal. In order to clarify the situation in the studied material, the distribution in the size of the grains was investigated. The study revealed that the particle size distribution covers the range from 0.95 to 240 μm, and particles with sizes outside the aforementioned range were not detected. The resulting distribution can be characterized by a broad Gaussian distribution peaked at 65μm and with a half-width of 135 μm. The result suggests that a statistically insignificant number of grains may have dimensions comparable to the correlation length at the critical temperature, the magnitude of which is estimated below. In addition, the specific heat calculated numerically for finite 1D clusters[20] confirmed that in the vicinity of the broad maximum, the difference in the specific heat of a cluster containing $N=11$ spins and the specific heat estimated in the thermodynamic limit is much smaller than the deviation of observed in the experimental results and considered in the theoretical models. Consequently, it may be assumed that powder nature of the studied sample will not have pronounced effects on the specific heat data. This assumption was verified by a specific heat study from 0.4 to 3 K using a bundle of small single crystals. The comparison of the data obtained with the powder and the single crystals is presented in Fig. 7 and confirms the size sensitivity of the critical behavior on the dimensions of the grains. In contrast, the powder nature of the sample does not seem to be significant in the region of short-range ordering. Therefore, the finite dimensions of the grains do not seem to represent the main mechanism leading to the discrepancy between the data and the theoretical models.

It may be assumed that spatial anisotropy of the exchange interaction could contribute to the deviation of the specific heat data from the aforementioned limiting models. Unlike the susceptibility, the value of the specific heat maximum represents a constant which is characteristic for each theoretical model. Therefore it seems that specific heat may be more sensitive to the potential presence of spatial anisotropy in the

exchange interaction. However, without corresponding theoretical predictions, the character of the spatial anisotropy can only be qualitatively estimated. The results of the analysis of the susceptibility and magnetization suggest that $Cu(H_2O)_2(en)SO_4$ behaves similar to a 2D HAF on a square lattice. Consequently, it may be expected that the exchange coupling mediated by the hydrogen bonds will be much stronger than that mediated by the covalent bonds in the $[SO_4]^{2-}$ unit, i.e., $J_2 \gg J_1$. This possibility is further supported by the low-temperature ESR study, where the unpaired electron was found to be described by the wave function with $d_{x^2-y^2}$ symmetry. The same conclusion is also drawn from a study comparing the present results with those obtained from $Cu(H_2O)_2(phen)SO_4$, a material with bond lengths and angles in the linking $[SO_4]^{2-}$ unit nearly identical to those in $Cu(H_2O)_2(en)SO_4$, but with an altered network of hydrogen bonds.[32] The fact that changing the arrangement and strength of the hydrogen bonds leads to a significant decrease of the exchange interaction in $Cu(H_2O)_2(phen)SO_4$ supports the minor role of the $[SO_4]^{2-}$ unit in mediating the exchange coupling.

When considering the weak hydrogen bonds between the layers, it might be assumed that the interlayer exchange interaction can be responsible for the onset of long-range order. The degree of isolation of the layers is manifested in the value of the intralayer correlation length ξ at the critical temperature. The correlation length exponentially increases at low temperatures and may be written as[25]

$$\frac{\xi}{a} = \frac{e}{8}\frac{c/a}{2\pi\rho}\exp\left(\frac{2\pi\rho}{T}\right)\left[1 - 0.5\frac{T}{2\pi\rho} + O\left(\frac{T}{2\pi\rho}\right)^2\right], \quad (3)$$

where $c = 1.657Ja$ and $\rho = 0.18J$ (Ref. 33) represent the normalized spin-wave velocity and spin-stiffness constants, respectively, and a stands for the lattice parameter. For $Cu(H_2O)_2(en)SO_4$, the correlation length at the critical temperature is found to be $\xi/a \approx 14$ (Ref. 34). For a pure 2D Heisenberg antiferromagnet with weak interlayer coupling, true 3D ordering occurs at the temperature given approximately by the criterion[35]

$$T_N \approx J'(\xi/a)^2. \quad (4)$$

Using this expression, with $\xi/a = 14$ and $T_N = 0.91$ K, yields $J'/k_B \approx 4.5$ mK. The high ratio between intralayer and interlayer couplings ($J/J' \approx 300$) confirms the weakness of the hydrogen bonds between the layers.

The resulting value of J' is comparable with the magnitude of the dipolar coupling between Cu(II) ions from adjacent layers $J^{dip} \approx 3$ mK. The comparison suggests that both the interlayer exchange interaction and the dipolar coupling contribute to the onset of long-range ordering at $T_N = 0.91$ K.

V. CONCLUSIONS

Herein, we presented a detailed study and analysis of the structure, thermodynamic properties, and magnetic resonance of $Cu(H_2O)_2(en)SO_4$. The results of the analyses of the thermodynamic quantities and ESR spectra, together with the comparative study of $Cu(H_2O)_2(phen)SO_4$,[32] suggest that $Cu(H_2O)_2(en)SO_4$ represents a quasi-two-dimensional $S = 1/2$ Heisenberg antiferromagnet with pronounced spatial anisotropy of its exchange interaction. More specifically, the fact that the magnetic properties can be reasonably approximated by predictions for an $S = 1/2$ 2D Heisenberg antiferromagnet on a square lattice confirms that exchange coupling ($J/k_B = -1.4$ K) is mediated predominantly by a square network of hydrogen bonds, whereas the $[SO_4]^{2-}$ unit plays only a minor role. Consequently, $Cu(H_2O)_2(en)SO_4$ might be located in the region of the phase diagram where collinear Néel-type ordering, characteristic for nonfrustrated and partially frustrated lattices, persists in the ground state.

The interlayer exchange interaction and dipolar coupling are proposed to be responsible for the long-range magnetic ordering observed at $T_N = 0.91$ K. The estimated ratio of the intralayer and interlayer exchange couplings suggests that $Cu(H_2O)_2(en)SO_4$ can be considered as a material appropriate for experimental studies of 2D Heisenberg magnets.

Although a systematic study of the correlation between the energy of the hydrogen bonds and the spatial arrangement of the participating atoms has been conducted,[14] to our knowledge, little is known about the possibilities of tuning the exchange coupling via hydrogen bonds. On the other hand, the role of the $[SO_4]^{2-}$ unit and the hydrogen bonds in mediating the exchange coupling could be clarified by systematic studies of the structural and thermodynamic properties of materials from the $Cu(H_2O)_2(X)SO_4$ series (X = imidazole, bipyridine, nicotinamide). Obviously, the existence and the strength of the hydrogen bonds will be influenced by the volume and the type of the X unit. In addition, if a smaller distortion of the octahedron is achieved, then enhanced exchange coupling along the chains can be expected. This enhancement will occur because the unpaired electron from Cu(II) ion will occupy the d_{z^2} orbital with higher probability. Alternatively, in compounds from the $Ni(H_2O)_2(X)SO_4$ class, if successfully synthesized, such an enhancement should be apparent since, for a Ni(II) ion in octahedral surroundings, the two unpaired electrons occupy both the $d_{x^2-y^2}$ and the d_{z^2} orbitals. If the modification of the exchange couplings in the various directions can be successfully achieved in the aforementioned way, then it will provide a means to change the position of the studied material in the phase diagram proposed for the systems described by the Row model. This interesting possibility is worthy of additional experimental effort.

ACKNOWLEDGMENTS

We thank D. Stratakis for early contributions to this work. We are grateful to M. Kušnierova for conducting the particle size analysis. This work was supported, in part, by VEGA Grant No. 1/0430/03, by the National Science Foundation via Grant Nos. INT-0089140 and DMR-0305371, and by APVT Project No. 20-009902. Material support from U.S. Steel DZ Energetika is gratefully acknowledged.

[1] P. Schiffer and A. Ramirez, Comments Condens. Matter Phys. **18**, 21 (1996), and references therein.
[2] L. Cappriotti, A. E. Trumper, and S. Sorella, Phys. Rev. Lett. **82**, 3899 (1999).
[3] P. Fazekas and P. W. Anderson, Philos. Mag. **30**, 423 (1974).
[4] U. Bhaumik and I. Bose, Phys. Rev. B **58**, 73 (1998).
[5] A. E. Trumper, Phys. Rev. B **60**, 2987 (1999).
[6] Z. Weihong, R. H. McKenzie, and R. R. P. Singh, Phys. Rev. B **59**, 14 367 (1999).
[7] K. Hirota, Y. Nakazawa, and M. Ishikawa, J. Magn. Magn. Mater. **90 & 91**, 279 (1990).
[8] M. Suzuki, I. Yamada, H. Kadowaki, and F. Takei, J. Phys.: Condens. Matter **5**, 4225 (1993).
[9] J. N. Reimers, R. Dahn, J. E. Greedan, C. V. Stager, G. Liu, I. Davidson, and U. von Sacken, J. Solid State Chem. **102**, 542 (1993).
[10] M. Tamura and R. Kato, J. Phys.: Condens. Matter **14**, L729 (2002).
[11] H. Seo and H. Fukuyama, J. Phys. Soc. Jpn. **67**, 1848 (1998).
[12] J. M. Williams, J. R. Ferraro, R. J. Thorn, K. D. Carlson, U. Geiser, H. H. Wang, A. M. Kini, and M. H. Whangbo, *Organic Superconductors, Synthesis, Structure, Properties and Theory* (Prentice Hall, Englewood Cliffs, NJ, 1992).
[13] V. Manríquez, M. Campos-Valette, N. Lara, N. González-Tejeda, O. Wittke, G. Díaz, S. Diez, R. Muñoz, and L. Kriskovic, J. Chem. Crystall. **26**, 15 (1996).
[14] G. R. Desiraju and T. Steiner, *The Weak Hydrogen Bonds in Structural Chemistry and Biology* (Oxford Science Publications, Oxford, 1999).
[15] M. B. Stone, Y. Chen, J. Rittner, H. Yardimci, D. H. Reich, C. Broholm, D. V. Ferraris, and T. Leitka, Phys. Rev. B **65**, 064423 (2002).
[16] R. Tiron, W. Wernsdorfer, N. Alinga-Alcade, and G. Christou, Phys. Rev. B **68**, 140407 (2003).
[17] M. W. Meisel, G. R. Stewart, and E. D. Adams, Cryogenics **29**, 1168 (1989).
[18] M. Orendáč, Ph.D. thesis, P. J. Šafárik University, 1996.
[19] H. Mori, S. Tanaka, and T. Mori, Phys. Rev. B **57**, 12 023 (1998).
[20] J. C. Bonner and M. E. Fischer, Phys. Rev. **135**, A640 (1964).
[21] H. A. Algra, L. J. de Jongh, and R. L. Carlin, Physica B **93**, 24 (1978).
[22] N. Elstner, R. R. P. Singh, and A. P. Young, Phys. Rev. Lett. **71**, 1629 (1993).
[23] R. B. Griffiths, Phys. Rev. **133**, A768 (1964).
[24] M. E. Zhitomirsky and T. Nikuni, Phys. Rev. B **57**, 5013 (1998).
[25] F. M. Woodward, A. S. Albrecht, C. M. Wynn, C. P. Landee, and M. M. Turnbull, Phys. Rev. B **65**, 144412 (2002).
[26] H. W. J. Blöte, Physica B **79**, 427 (1975).
[27] L. J. de Jongh and A. R. Miedema, Adv. Phys. **23**, 2 (1974).
[28] A. Cuccoli, T. Roscilde, V. Tognetti, R. Vaia, and P. Verrucchi, Phys. Rev. B **67**, 104414 (2003).
[29] A. Orendáčová, D. Horváth, M. Orendáč, E. Čižmár, M. Kačmár, V. Bondarenko, A. G. Anders, and A. Feher, Phys. Rev. B **65**, 014420 (2001).
[30] A. G. Anders, S. V. Volotskii, S. V. Startsev, A. Feher, and A. Orendacheva, Low Temp. Phys. **21**, 52 (1995).
[31] C. M. Wynn, M. A. Girtu, and W. B. Brinckerhoff, Chem. Mater. **9**, 2156 (1997).
[32] M. Kajňaková, A. Orendáčová, M. Orendáč, J.-H. Park, O. V. Kravchyna, A. G. Anders, J. Černák, A. Feher, and M. W. Meisel, J. Magn. Magn. Mater. **272-276**, 867 (2004).
[33] B. B. Beard, R. J. Birgeneau, M. Greven, and U. J. Wiese, Phys. Rev. Lett. **80**, 1742 (1998).
[34] It should be noted that ξ/a was evaluated using $c'=2c$ and $\rho'=2\rho$ due to the $2J$ term in the Heisenberg Hamiltonian from which specific heat and susceptibility for the 1D and 2D systems were calculated.
[35] S. Chakravarty, B. I. Halperin, and D. R. Nelson, Phys. Rev. Lett. **60**, 1057 (1988).